REVISION 2

Developing vanadium valence state oxybarometers (spinel-melt, olivine-melt, spinel-olivine) and V/(Cr+Al) partitioning (spinel-melt) for martian olivine-phyric basalts

J.J. Papike[1] (jpapike@unm.edu), P.V. Burger[1], A.S. Bell[1], L. Le[2], C.K. Shearer[1], S.R. Sutton[3], J. Jones[4], and M. Newville[3]

[1]Institute of Meteoritics, Department of Earth and Planetary Sciences,
University of New Mexico, Albuquerque New Mexico 87131,

[2]ESCG, Houston, TX 77058,

[3]Center for Advanced Radiation Sources, University of Chicago, Chicago, Illinois 60637

[4]NASA/Johnson Space Center, Houston, TX 77058

ABSTRACT

A spiked (with REE, V, Sc) martian basalt Yamato 980459 (Y98) composition was used to synthesize olivine, spinel, and pyroxene at 1200˚C at five oxygen fugacities: IW-1, IW, IW+1, IW+2, and QFM. These run products were analyzed by electron microprobe, ion microprobe, and x-ray absorption near-edge spectroscopy to establish four oxybarometers based on vanadium partitioning behavior between the following pairs of phases: V spinel-melt, V/(Cr+Al) spinel-melt, olivine-melt, and spinel-olivine. The results for the spinel-melt, olivine-melt, and V/(Cr+Al) spinel-melt are applicable for the entire oxygen fugacity range while the spinel-olivine oxybarometer is only applicable between IW-1 and IW+1. The oxybarometer based on V partitioning between spinel-olivine is restricted to basalts that crystallized under low oxygen fugacities, some martian, all lunar, as well as samples from 4 Vesta. The true potential and power of the new spinel-olivine oxybarometer is that it does not require samples representative of a

melt composition or samples with some remnant of quenched melt present. It just requires that the spinel-olivine pairs were in equilibrium when the partitioning of V occurred. We have applied the V spinel-olivine oxybarometer to the Y98 meteorite as a test of the method.

INTRODUCTION

The studies of Herd et al. (2002), Herd (2003), Wadhwa (2001), and Goodrich et al. (2003) demonstrated that the oxygen fugacity in martian basalts varies up to four log units and is correlated with geochemical parameters such as LREE/HREE and $^{87}Sr/^{86}Sr$. These correlations have been interpreted to indicate the presence of reduced, incompatible-element-depleted and oxidized, incompatible-element-enriched reservoirs that were produced during the early stages of martian differentiation (~4.5 Ga) (Herd et al. 2002; Herd 2003; Wadhwa 2001; Goodrich et al. 2003; Shih et al. 1982; Borg et al. 1997; Jones 2003). Martian basaltic magmatism as it is represented by the shergottites is thought to be characterized by mixing between these two reservoirs. Early studies estimated oxygen fugacity by two independent approaches, fO_2 from mineral equilibria (Herd et al. 2002; Herd 2003; Goodrich et al. 2003) or multivalent behavior of Eu in phases such as pyroxene bulk-rock elemental-isotopic measurements (Wadhwa 2001). The work of Shearer et al. (2006) used a different approach to evaluate the fO_2 of potential reservoirs that occur in the martian mantle. In that paper, we used the estimated V content of the near-primary martian basalt melt Yamato 980459 (Y98) and the V content of one of the earliest phases to crystallize from this basalt (olivine). This approach, however, is somewhat compromised as the composition of the coexisting liquid must be inferred indirectly. In this work we use a different approach that is based on the partitioning of V between olivine and spinel. When using this approach, it is of paramount importance to identify equilibrium spinel-olivine

pairs. A criterion to make this identification is also included in the discussion of the following sections.

EXPERIMENTAL

Experiments were prepared in a 1-atm Deltech gas mixing furnace. These runs were made using a spiked composition of martian meteorite Y98. The REEs were added as 0.6 wt.% of their oxides (Ce as CeO_2). Scandium and V were added as Sc_2O_3 and V_2O_3 and doped to 0.1 wt.%. Experimental charges of the Y98 composition were pasted onto Re-wire loops at imposed oxygen fugacities of IW-1, IW, IW+1, IW+2, and QFM. All experiments were held for 8 hours at 1500°C to ensure homogeneity and fO_2 equilibration. Charges were then cooled at 1000°C/hr to 1400, 1300 and 1200°C, and held at the final temperature for at least 48 hours, then drop-quenched into water. For experiments conducted at QFM, pressed pellet charges of Y98 were placed onto $Pt_{90}Rh_{10}$ loops and then air-quenched at the end of the same thermal history as the other fO_2 experiments. The Pt-wire loop does not oxidize at high fO_2, whereas the Re-wire loop prevents Fe loss at low fO_2. Analyses of the run products from the 1200°C experiments and phases in meteorite Y98 are presented in Table 1. The 1200°C temperature was used because we found that for our bulk composition, this is the optimal temperature to have spinel, olivine, pyroxene, and melt in equilibrium.

ANALYTICAL

Electron microprobe (EPMA)

Samples were initially analyzed using the Cameca SX100 at Johnson Space Center. Later analyses were collected on the JEOL JXA 8200 electron microprobe at the Institute of Meteoritics (IOM) and Department of Earth and Planetary Sciences (E&PS), at the University of New Mexico (UNM). Electron microprobe analyses initially examined the major/minor element

chemistry of the experiments and phases of interest (olivine, spinel, and glass). Samples were analyzed under a 15 kV accelerating voltage, 20 nA beam current, and a 2 μm spot for olivine, 10 μm for glass and <μm for spinel. Elements were calibrated using C.M. Taylor Co. EPMA standards, as well as additional standards developed in-house. Subsequent olivine measurements were focused on the trace element abundance of V in olivine. These measurements consisted of extended peak and background counting times for V in olivine, along with the concurrent measurement of Ti concentration. By increasing the counting statistics for both V and Ti (with the Ti Kβ peak representing a known interference for V Kα), the 3σ detection limit for each was reduced drastically (33 and 42 ppm for V and Ti, respectively). The data is presented in Table 1 in an abbreviated fashion for space considerations. Complete data sets for spinel, olivine, and glass are given in the electronic appendices.

Ion microprobe (SIMS)

Vanadium measurements for olivine in the Y98 meteorite sample were collected on the Cameca 4f Ion Microprobe in the Institute of Meteoritics at the University of New Mexico. Analytical conditions included an accelerating voltage of 10 kV, a beam current of 20 nA, and an offset voltage of -105 V. Standardization was carried out using 3 olivines and 1 orthopyroxene standard. See Shearer et al. (2006) for details.

Error analyses of data and partition coefficients

See appendix for details.

X-ray Absorption Near Edge Spectroscopy (XANES) data acquisition and reduction

Vanadium K-edge XANES data was acquired with the x-ray microprobe at GSECARS beamline 13-ID at the Advanced Photon Source (APS), Argonne National Laboratory, Illinois. The x-ray source at APS beamline 13-ID was a 72-pole 33mm period undulator. Beam focusing

was accomplished with dynamically-figured Kirkpatrick-Baez focusing mirrors; this configuration yielded a beam focused to a final spot size of ~4 μm^2. All spectra were acquired in fluorescence mode utilizing a Si(311) monochromater and a silicon-drift solid state detector offset at a 45° angle from the sample. Spectra were collected through the energy range of 5415 eV to 5670 eV. Energy calibration was accomplished using metallic V foil. The energy step width was set to 0.2 eV in the pre-edge/near-edge region and 4 eV in the far pre-edge and far post-edge spectral regions. Data acquisition consisted of three spectral sweeps per spot analysis. The three resultant spectra were subsequently merged into a single spectrum. Multiple olivine crystals were analyzed in each experimental charge. A total of four to five olivine spot analyses were obtained for each experimental charge. Vanadium valence was quantified using the intensity of the V pre-edge with the methodology and calibration described by Sutton et al. (2005). The V valence results are illustrated in Figure 1.

RESULTS AND DISCUSSION

Spinel-melt partitioning of vanadium as a function of oxygen fugacity

Our first effort using spinel as an indicator of relative oxygen fugacity (Papike et al. 2004) was only qualitative. That study showed that using only zoned spinel, relative oxygen fugacities can be estimated. Our first insights into this technique resulted from acquiring EPMA traverses across spinel grains from core to rim on grains that showed zoning from chromite to ulvospinel. The zoning profiles showed the normal trends of core to rim decreases of Cr, Al, and Mg and increases of Fe, Ti, and Mn. However, the behavior of V is very different when comparing terrestrial basalts and lunar basalts with V behavior in martian basalts, falling somewhere in between these two end-members. In terrestrial basaltic liquids, $V^{4+} > V^{3+}$, whereas in lunar basalts $V^{3+} > V^{4+}$, and in martian basalts V^{3+} and V^{4+} are both significant. The trends

(core to rim) for the Moon show a strong positive correlation of V and Cr and negative correlation of V and Ti. For the Earth, the trends are just the opposite, with a strong negative correlation of V and Cr and strong positive correlation of V and Ti. Chromite in martian basalts shows trends in between. These systematics show that at high oxygen fugacity (Earth), V^{4+} follows Ti^{4+}, whereas at low oxygen fugacity (Moon), V^{3+} follows Cr^{3+}. In this paper, we convert the V/(Cr+Al) systematics in spinel from a qualitative oxybarometer to a quantitative one by using our new experimental data for five oxygen fugacities.

The spinel oxybarometer (e.g. Canil 2002) is very useful, but requires equilibrium pairs of coexisting spinel and melt. Results from this study are shown in Figure 2a and are compared to the results of Canil (2002). We note that the trend of our data agrees very well with Canil's (2002) results for high Cr/Al spinel. Figure 2d normalizes the $D_V^{spinel/melt}$ to the ferric iron content of the spinel. The increase in ferric iron with oxygen fugacity steepens the negative slope from left to right. The significant increase in $D_V^{spinel/melt}$ with decreasing oxygen fugacity is a result of the strong structural preference for V^{3+} vs. V^{4+}. Canil (2002) shows the strong dependence of $D_V^{spinel/melt}$ on the Al content of the spinel. High Al/Cr spinels have a much lower site preference for V^{3+} than high Cr/Al spinels. This is because V^{3+} and Cr^{3+} are very similar geochemically and have high crystal field stabilization energy in octahedral coordination (Papike et al. 2005). Additionally the behavior of Cr^{3+} and V^{3+} are highly correlated because of their similar ionic radii and identical charge. Papike et al. (2005) also showed that V^{3+} enters spinel in the "normal" spinel atomic arrangement, whereas V^{4+} enters in the "inverse" arrangement. The mixed domains of "normal" and "inverse" will have an effect on the partition coefficient values for V and might explain the complicated trajectory of the $D_V^{spinel/\ melt}$ vs. fO_2 (Fig. 2a). This trajectory is found in both the study by Canil (2002) and the present study.

Vanadium olivine-melt partitioning as a function of oxygen fugacity

Our results using V in olivine as an oxybarometer (Shearer et al. 2006) gave an estimated oxygen fugacity of crystallization for Y98 of IW+0.9. The application of this oxybarometer requires the presence of melt in the meteorite or a bulk rock composition that is a melt composition. Our current study adds data from experiments at two additional oxygen fugacities. An important paper (Mallman and O'Neill, 2013) has also recently calibrated an empirical thermometer and oxybarometer based on V and Sc partitioning between olivine and melt (IW+1 and IW+2) to the Shearer et al. 2006 calibration. The results for both studies are in agreement and demonstrate that the high spike levels of REE in the present study had no apparent effect on V partitioning between olivine and melt. The increasing $D_V^{olivine/melt}$ with decreasing fO_2 is attributed to the increase of V^{3+}/V^{4+} in the melt (see Fig. 1 and 2c). The XANES data (Fig. 1) shows that at fO_2<IW+2, all of the V that enters the olivine is trivalent. The greater compatibility of V^{3+} over V^{4+} is not due to size, as the radii of both are comfortable in the olivine octahedral sites. Rather, it is due to charge balance, because for every V^{3+} cation that enters the olivine structure, one vacancy is required, whereas for V^{4+}, two vacancies are required (Papike et al. 2005). The rate of increase of D_V (with decreasing oxygen fugacity) is greater for olivine than spinel and therefore the $D_V^{spinel/olivine}$ starts decreasing at fO_2<IW+1 and thus makes the spinel/olivine oxybarometer possible.

Vanadium spinel-olivine partitioning as a function of oxygen fugacity

We have been searching for an oxybarometer with application to olivine-phyric and lherzolitic martian basalts that does not require the presence of melt. One possible solution to this quandary is to use partitioning of V between spinel and olivine. Both are near liquidus phases in these compositions and commonly share grain contacts. We examined the partitioning of V

between spinel and olivine and the results are shown in Figure 2e. Note that the spinel/olivine partitioning of V provides a powerful oxybarometer at low oxygen fugacities, over two orders of magnitude, from IW-1 to IW+1. Many of the olivine-phyric martian basalts fall in this range. We have selected one martian meteorite to test our V spinel/olivine oxybarometer, Y98. The modes and mineral chemistry of the phases present in this meteorite are discussed in detail, in Papike et al. (2009) and Meyer (2013). The true potential and power of the new spinel-olivine oxybarometer is that it does not require samples representing melts or samples with remnant melt present. It simply requires that the spinel-olivine pairs co-crystallized from the liquid and are therefore in equilibrium. An effective way to discriminate between multiple olivine-spinel pairs is to calculate the molar Mg-Fe^{2+} exchange $K_d=(X_{Mg}/X_{Fe2+})_{olivine}(X_{Fe2+}/X_{Mg})_{spinel}$ of ~4.4-5.6 (determined from our 1200˚C experimental data for bulk runs). See Roeder et al. (1979), and references therein, for background on this K_d. Our spinel-olivine mineral pair had a K_d of 4.2 which is consistent with the established equilibrium range. Plotting this pair on the diagram illustrated in Figure 2e yields an estimated oxygen fugacity of IW+0.8. The chemical compositions for spinel and olivine for Y98 is presented in Table 1. Early results of this study are presented in Papike et al. (2013).

V/(Cr+Al) partitioning between spinel-melt as a function of oxygen fugacity

With our new experimental data discussed in this paper we are able to further develop our previous qualitative spinel oxybarometer (Papike et al. 2004, 2005). The experimental V/(Cr+Al) data (elemental wt.%) for spinel is given Table 1. This same ratio is given for the coexisting glass in Table 1. Figure 2b displays [$V/(Cr+Al)^{spinel}$ / $V/(Cr+Al)^{bulk\ experimental\ melt}$] as a function of oxygen fugacity. Once calibrated for the appropriate melt composition and approximate temperature of spinel crystallization, this oxybarometer is easy to use because it requires only the

186 earliest spinel composition (core, high Mg) that is in equilibrium with the appropriate melt
187 composition. It can be used for oxygen fugacities between IW-1 and QFM.

188 **CONCLUDING STATEMENT**

189 We calibrated 4 oxybarometers based on the multivalent behavior of V for a Y98 proxy
190 composition. We applied all four to meteorite Y98 and our estimated oxygen fugacity is IW+0.8
191 to IW+1.6. This range should be considered the window of possible oxygen fugacities for
192 meteorite Y98. This should also be considered our best estimate of oxygen fugacity for Y98 to
193 date. These results are most useful to researchers investigating the oxygen fugacities of and
194 implications for martian rocks, especially those that were likely derived from the martian mantle
195 (e.g. Yamato 980459).

196 **REFERENCES CITED**

197 Borg, L.E., Nyquist, L.E., Weismann, H., and Shih, S.-Y. (1997) Constraints on martian
198 differentiation process from Rb-Sr and Sm-Nd isotopic analyses of basaltic shergottite
199 QUE94201. Geochimica et Cosmochimica Acta, 61, 4915-4931.
200 Canil, D. (2002) Vanadium in peridotites, mantle redox states and tectonic environments:
201 Archean to present. Earth and Planetary Science Letters, 195,75-90.
202 Droop, G.T.R. (1987) A general equation for estimating Fe3+ concentrations in ferromagnesian
203 silicates and oxides from microprobe analyses, using stoichiometric criteria.
204 Mineralogical Magazine 51, 431–435.
205 Goodrich, C.A., Herd, C.D.K., and Taylor, L. (2003) Spinels and oxygen fugacity in olivine-
206 phyric and lherzolitic shergottites. Meteoritics and Planetary Science, 38, 1773-1792.
207 Herd, C.D.K. (2003) The oxygen fugacity of olivine-phyric martian basalts and the components
208 within the mantle and crust of Mars. Meteoritics and Planetary Science, 38, 1793-1805.

Herd, C.D.K., Borg, L., Jones, J.H., and Papike, J.J. (2002) Oxygen fugacity and geochemical variations in martian basalts: Implications for martian basalt petrogenesis and the oxidation of the upper mantle of Mars. Geochimica et Cosmochimica Acta, 66, 2025-2036.

Jones, J.H. (2003) Constraints on the structure of the martian interior determined from chemical and isotopic signatures of SNC meteorites. Meteorites and Planetary Science, 38, 1807-1814.

Mallmann, G, and H. O'Neil (2013) Calibration of an empirical thermometer and oxybarometer based on partitioning on Sc, Y, and Y between olivine and silicate melt. Journal of Petrology, 1-17

Meyer, C. (2013) The Mars Meteorite Compendium. Available from: http://curator.jsc.nasa.gov/antmet/mmc/.

Papike, J.J., Karner, J.M., and Shearer, C.K. (2004) Comparative planetary mineralogy; V/(Cr +Al) systematics in chromite as an indicator of relative oxygen fugacity. American Mineralogist 89, 1557-1560.

Papike, J.J., Karner, J.M., and Shearer C.K. (2005) Comparative planetary mineralogy: Valence state partitioning of Cr, Fe, Ti, and V among crystallographic sites in olivine, pyroxene, and spinel from planetary basalts. American Mineralogist, 90, 277-290.

Papike, J.J., Karner, J.M, Shearer, C.K., and Burger, P.V. (2009) Silicate mineralogy of martian meteorites. Geochimica et Cosmochimica Acta, 73, 7443-7485.

Papike, J.J., Le, L., Burger, P.V., Shearer, C.K., Bell, A.S. and Jones, J. (2013) A new spinel-olivine oxybarometer: Near-liquidus partitioning of V between olivine-melt, spinel-melt,

and spinel-olivine in martian basalt composition Y980459 as a function of oxygen fugacity. 44th Lunar and Planetary Science Conference, Abs. #1087, Houston.

Roeder, P.L., Campbell, I.H., and Jamieson, H.E. (1979) A re-evaluation of the olivine- spinel geothermometers. Contributions to Mineralogy and Petrology, 68, 325-334.

Shearer, C.K., McKay, G., Papike, J.J., and Karner, J.M. (2006) Valence state partitioning of vanadium between olivine-liquid: Estimates of oxygen fugacity of Y980459 and application to other olivine-phyric martian basalts. American Mineralogist, 91, 1657-1663.

Shih, C.-Y., Nyquist, L.E., Bogard, D.D., McKay, G.A., Wooden, J.L., Bansal, B.M. (1982) Chronology and petrogenesis of young achondrites, Shergotty, Zagami, and ALHA77005: Late magmatism on a geologically active planet. Geochimica et Cosmochimica Acta, 46, 2323-2344.

Sutton, S.R., Karner, J., Papike, J., Delaney, J.S., Shearer, C., Newville, M., Eng, P., Rivers, M., and Dyar, M.D. (2005) Vanadium K edge XANES of synthetic and natural basaltic glasses and application to microscale oxygen barometry. Geochimica et Cosmochimica Acta, 69, 2333-2348.

Wadhwa, M. (2001) Redox state of Mars' upper mantle from Eu anomalies in shergottite pyroxene. Science, 292, 1527-1530.

ACKNOWLEDGEMENTS

This research was supported by NASA Cosmochemistry grants to C. Shearer and J. Jones. XANES spectra were collected at GeoSoilEnviroCARS(sector 13) Advanced Photon Source (APS), Argonne National Laboratory. We gratefully acknowledge the beamline award, as well as assistance of beamline staff. GeoSoilEnviroCARS is supported by the National Science

Foundation-Earth Sciences (EAR-1128799) and Department Geosciences (DE-FG02-94ER14466). Use of the Advanced Photon Source was supported by U.S. Department of Energy. Office of Science. Office of Basic Energy Science under contract No. DE-AC02-06CH11357.

FIGURE CAPTIONS

Figure 1. Stacked XANES spectra comparing the V pre-edge feature in olivine, across the range of oxygen fugacities imposed on the experiments. This diagram shows the preference of V^{3+} over V^{4+}. See discussion above. V^{4+} will not enter the olivine structure until the melt is highly enriched in V^{4+}.

Figure 2. In all cases, the error bars represent the 1σ propagated error. See appendix for further discussion. (a) Spinel partition coefficients across the oxygen fugacity spectrum. Mean V in spinels vs. glass; Canil (2002) data for comparison. There are two spinel populations in the IW+1 and IW+2 experiments; the higher V population only is used for the purpose of producing the curve, as this is the group that is inferred to be in equilibrium with the melt. The Y98 meteorite analysis represents the most Mg-rich spinel divided by bulk meteorite data from Meyer (2013). (b) V/(Cr+Al) in spinel verses oxygen fugacity (in elemental wt.%). As with Figure 2a, only the higher V population of spinel is used (for the IW+1 and IW+2) experiments. (c) Olivine partition coefficients across the oxygen fugacity spectrum. (d) The V in spinel-melt oxybarometer scaled to the ferric iron content of the spinel. (e) The new spinel/olivine oxybarometer plots V in spinel vs. V in olivine. A test point illustrating the V partitioning between Y98 meteorite spinel-olivine is shown as an application of the method. The blue band represents the range of oxygen fugacities estimated by our oxybarometers.

Table 1. Experimental average values. 1σ errors appear in parentheses.

	Spinel											
	IW-1 (Y98A18)		IW (Y98A15)		IW+1£ (Y98A19)		IW+2£ (Y98A20)		QFM (Y98A11)		Y98 Meteorite	
Element (ppm)												
Al	50763	(3174)	52259	(10688)	49470	(3537)	39636	(2180)	45985	(1276)	64442	(13593)
Mg	46926	(950)	45201	(2197)	41871	(631)	48117	(569)	47280	(933)	58386	(4467)
Fe^{2+}	172767	(2476)	180259	(3529)	184927	(3030)	168483	(2095)	168824	(1705)	169574	(5014)
Ti	6564	(1099)	9180	(2326)	7304	(759)	5030	(576)	5265	(259)	19173	(6821)
V	21160	(373)	19580	(1017)	19219	(1426)	12138	(662)	7689	(201)	3922	(745)
Cr	360583	(3280)	347530	(17440)	352675	(4061)	375341	(4893)	331609	(4976)	334356	(33850)
Fe^{3+} ¤	16170	(2455)	20610	(2342)	23244	(1712)	34523	(1484)	70656	(2647)	23889	(3488)

	Olivine											
	IW-1 (Y98A18)		IW (Y98A15)		IW+1£ (Y98A19)		IW+2£ (Y98A20)		QFM (Y98A11)		Y98 Meteorite	
Element (ppm)												
Al	285	(344)	200	(62)	223	(93)	320	(89)	198	(86)	180	(70)
Mg	223449	(1315)	222808	(1648)	229191	(7182)	238656	(1642)	233578	(729)	236856	(8739)
Fe^{2+}	187432	(1089)	195087	(750)	182441	(10726)	165508	(1846)	178191	(778)	164208	(12379)
Ti*	71	(17)	51	(19)	40	(12)	48	(16)	60	(12)	30	(29)
V*	343	(12)	227	(18)	159	(19)	128	(17)	81	(11)	35	(4)
Cr	2874	(79)	1662	(61)	1864	(281)	1564	(393)	628	(42)	2059	(586)

	Glass											
	IW-1 (Y98A18)		IW (Y98A15)		IW+1£ (Y98A19)		IW+2£ (Y98A20)		QFM (Y98A11)		Y98 Meteorite	
Element (ppm)												
Al	36312	(918)	39265	(393)	40786	(339)	35758	(2838)	36750	(276)	29003	
Mg	55750	(786)	53879	(561)	49623	(391)	60931	(662)	54141	(397)		
Fe^{2+}	140581	(1089)	144979	(1131)	142166	(1046)	137073	(1222)	138361	(971)		
Ti	4675	(177)	4846	(156)	5127	(180)	4345	(185)	4620	(171)		
V	700	(134)	763	(135)	746	(119)	864	(128)	803	(135)	188	
Cr	3515	(202)	2065	(200)	1328	(166)	1350	(167)	843	(163)	4807	

$D_V^{spinel/melt}$	30.22	25.67	25.76	14.05	9.57	20.86
$D_V^{olivine/melt}$	0.49	0.30	0.21	0.15	0.10	0.18
$D_V^{spinel/olivine}$	61.68	86.24	120.51	95.13	95.32	113.16
$K_d^{olivine\ x\ spinel}$	4.39	4.55	5.55	5.05	4.68	4.19
$(V)/(Cr+Al)^{spinel/melt}$	2.93	2.65	2.70	1.26	0.95	1.77
$Fe^{3+}/(Fe^{2+}+Fe^{3+})^{spinel}$	0.09	0.10	0.11	0.17	0.30	0.12

*Ti and V in olivine were measured using extended counting times on peaks and backgrounds to achieve a low detection limit, and to better characterize the Ti on V overlap. Vanadium in olivine from the Y98 meteorite was measured via SIMS.

¥Y98 meteorite glass values represent the bulk meteorite average values from Meyer (2013).

§Y98 meteorite spinel analysis represents the most Mg-rich spinel analyzed.

¤Estimated using the methodology of Droop (1987).

£Y98A19 and Y98A20 (IW+1 and IW+2 experiments, respectively) have two populations of spinels, the higher V population is presented here, and used in the plots in Figure 2. Average spinel as well as the lower V spinel population can be found in the appendices.

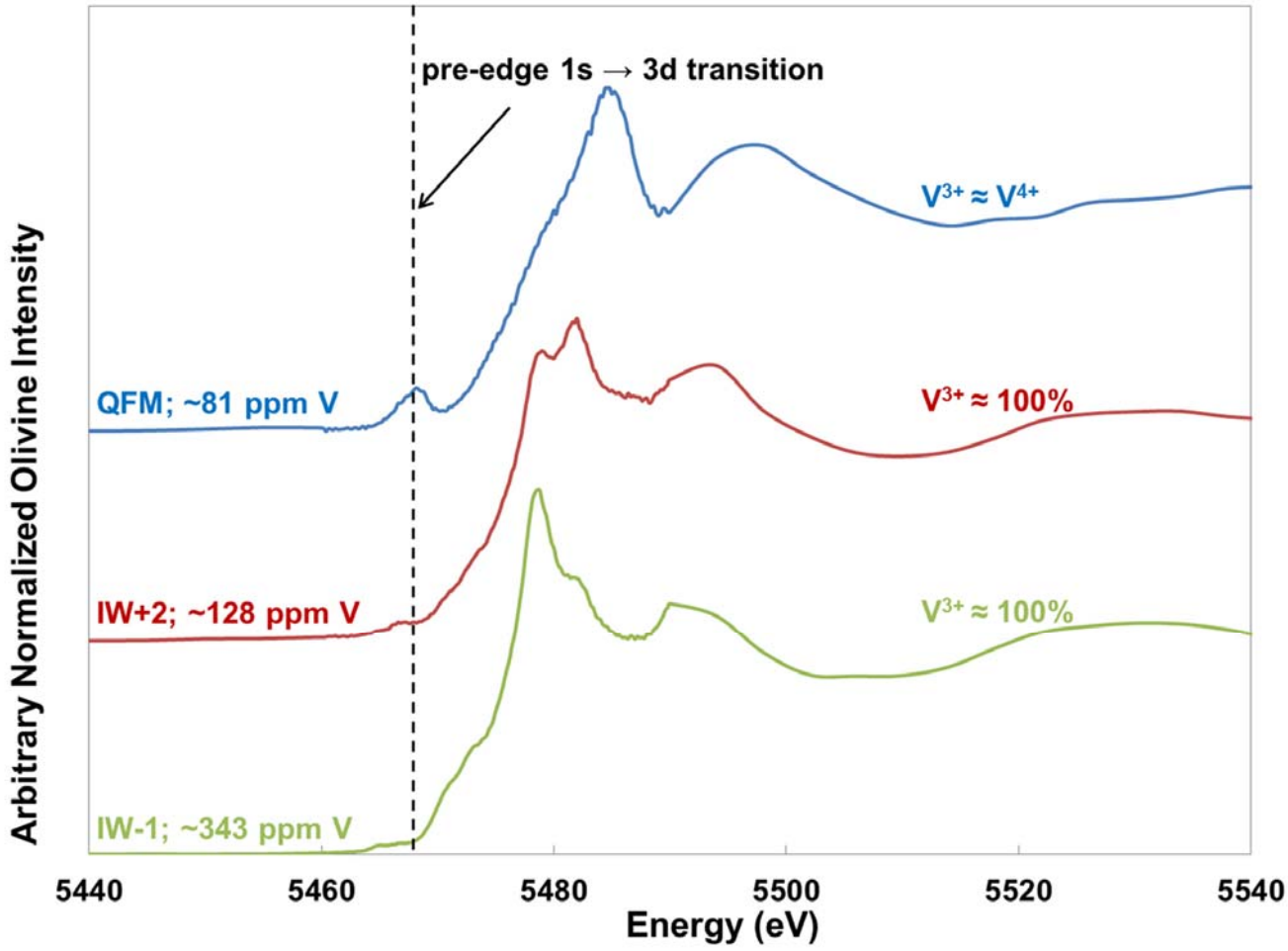
pre-edge 1s → 3d transition
V3+ ≈ V4+
QFM; ~81 ppm V
V3+ ≈ 100%
IW+2; ~128 ppm V
V3+ ≈ 100%
IW-1; ~343 ppm V
Arbitrary Normalized Olivine Intensity
5440
5460
5480
5500
5520
5540
Energy (eV)

Figure 2

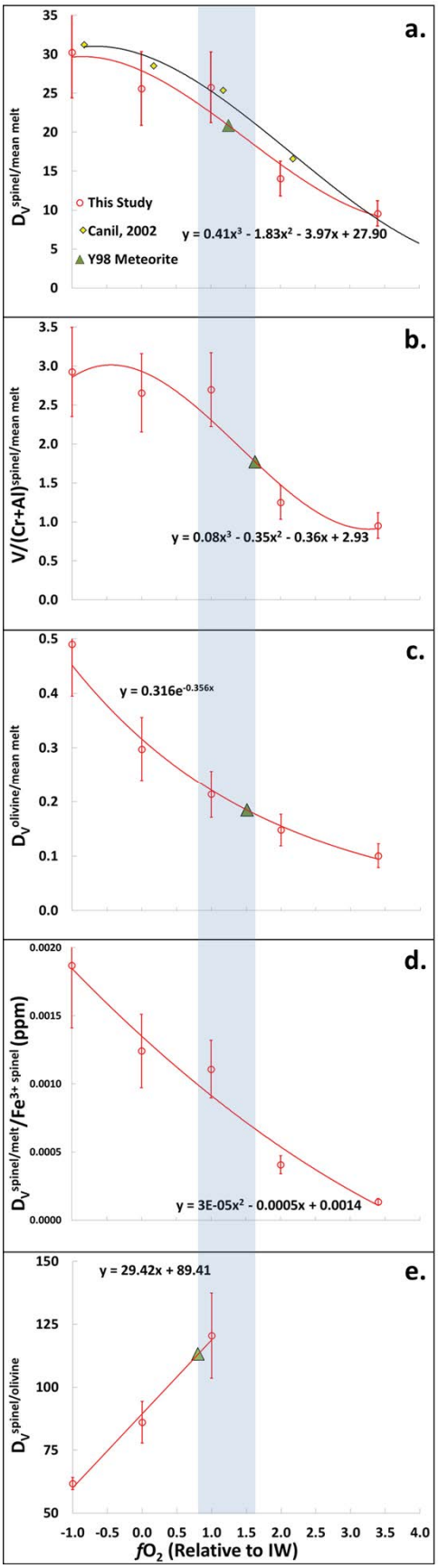
a.
D_V spinel/mean melt
This Study
Canil, 2002
Y98 Meteorite
y = 0.41x³ - 1.83x² - 3.97x + 27.90
b.
V/(Cr+Al)spinel/mean melt
y = 0.08x³ - 0.35x² - 0.36x + 2.93
c.
D_V olivine/mean melt
y = 0.316e^-0.356x
d.
D_V spinel/melt/Fe^{3+} spinel (ppm)
y = 3E-05x² - 0.0005x + 0.0014
e.
D_V spinel/olivine
y = 29.42x + 89.41
fO_2 (Relative to IW)